ACS Photonics

Letter

pubs.acs.org/journal/apchd5

Multipolar Coupling in Hybrid Metal–Dielectric Metasurfaces

Rui Guo,[†] Evgenia Rusak,[†,‡] Isabelle Staude,[*,†,§] Jason Dominguez,[⊥] Manuel Decker,[†] Carsten Rockstuhl,[‡,∥] Igal Brener,[⊥] Dragomir N. Neshev,[†] and Yuri S. Kivshar[†]

[†]Nonlinear Physics Centre and Centre for Ultrahigh Bandwidth Devices for Optical Systems (CUDOS), Research School of Physics and Engineering, The Australian National University, Canberra, ACT 2601, Australia

[‡]Institute of Theoretical Solid State Physics, Karlsruhe Institute of Technology, 76131 Karlsruhe, Germany

[§]Institute of Applied Physics, Abbe Center of Photonics, Friedrich-Schiller-Universität Jena, 07743 Jena, Germany

[⊥]Center for Integrated Nanotechnologies, Sandia National Laboratories, Albuquerque, New Mexico 87185, United States

[∥]Institute of Nanotechnology, Karlsruhe Institute of Technology, 76021 Karlsruhe, Germany

S *Supporting Information*

ABSTRACT: We study functional hybrid metasurfaces consisting of metal–dielectric nanoantennas that direct light from an incident plane wave or from localized light sources into a preferential direction. The directionality is obtained by carefully balancing the multipolar contributions to the scattering response from the constituents of the metasurface. The hybrid nanoantennas are composed of a plasmonic gold nanorod acting as a feed element and a silicon nanodisk acting as a director element. In order to experimentally realize this design, we have developed a two-step electron-beam lithography process in combination with a precision alignment step. The optical response of the fabricated sample is measured and reveals distinct signatures of coupling between the plasmonic and the dielectric nanoantenna elements that ultimately leads to unidirectional radiation of light.

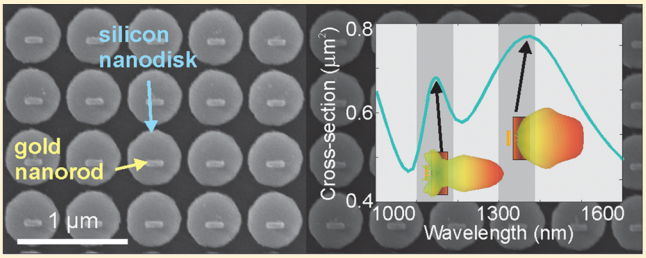

KEYWORDS: *metal–dielectric metasurfaces, subwavelength nanostructures, directional radiation properties, multipolar radiation*

Metasurfaces[1,2] that controllably direct light from an incident plane wave or from localized light sources are indispensable constituents for a future class of highly compact optical devices. They are made from designed meta-atoms that allow engineering the optical response of the metasurface toward a range of applications. While wavefront shaping is arguably the most intensively researched functionality of metasurfaces, they can also be tailored to provide an efficient link between localized optical near-fields and propagating optical far-fields, allowing for strong enhancement of light–matter interaction processes such as spontaneous emission enhancement, nonlinear optical processes, or perfect absorption in a small, defined volume. To this end, the metasurface can harness the abilities of nanoparticles to concentrate light into small volumes and to establish highly directional scattering patterns, thereby emitting or receiving light into or from a narrow solid angle efficiently. As such, the meta-atoms borrow their functionalities from optical nanoantennas including plasmonic and dielectric antennas. While plasmonic nanoantennas[3−6] have proven to provide good directionality and excellent coupling properties due to the strong field enhancement, they suffer from their intrinsic absorption.[7] All-dielectric nanoantennas,[8−12] on the other hand, exhibit high radiation efficiencies, but the lower field confinement also reduces coupling efficiencies. Hybrid metal–dielectric nanoantennas composed of plasmonic feed elements and dielectric director elements allow for combining the advantages of both plasmonic and all-dielectric nanoantennas. Hence, they may offer large Purcell enhancements and highly directional radiation patterns while preserving high radiation efficiencies at the same time. Various recent theoretical and numerical studies have analyzed hybrid nanoantenna architectures, mainly in the context of emission manipulation.[13−16] Typically, a resonant plasmonic dipole or feedgap antenna is used as a nanoantenna feed element, providing a strong near-field enhancement and thus a high enhancement of the radiative decay rate. Then, in order to shape the radiation pattern of the hybrid nanoantenna without introducing notable additional losses, a dielectric nanoantenna is employed as a director element. This allows us to capitalize on the strong field enhancement provided by the plasmonic feed element and, at the same time, to efficiently direct the emission in a specific direction. As a result, this sequential approach where near-field coupling between metallic and dielectric particles results in designed far-field radiation patterns can provide record values for directional emission enhancement from a dipole source that cannot be achieved with plasmonic or all-dielectric nanoantennas alone under the same conditions.[16] In addition to their prospective use for tailoring emission from

Received: January 7, 2016
Published: March 2, 2016

DOI: 10.1021/acsphotonics.6b00012
ACS Photonics 2016, 3, 349−353

nanoscopic sources, metal−dielectric nanoantennas can also offer very interesting opportunities for bidirectional scattering.[17,18] For example, coupling of a plasmonic antenna element (with a low quality factor) to a dielectric antenna element (with a high quality factor) allows combining resonances of very different quality factors and results in Fano resonances, which, in turn, can be used to achieve extended control over the directional radiation characteristics.[17,18]

Altogether, hybrid nanoantenna geometries are interesting candidates for a range of photonic applications, including directional nanoscale light sources,[13−16] biosensing,[19] and optical switching and routing.[20] By employing hybrid nanoantennas as meta-atoms for functional metasurfaces we, thereby, define a new type of *hybrid metasurfaces* with radiation properties defined by the properties of the underlying constituents. Since we use metal−dielectric nanoantennas as meta-atoms, these hybrid metasurfaces can provide new functionalities to realize directional and emission-shaping metasurfaces when, for example, quantum emitters are coupled to the plasmonic feed elements.[6,21] However, due to their structural complexity, the fabrication of resonantly coupled metal−dielectric metasurfaces is challenging and has not been demonstrated so far.

RESULTS AND DISCUSSION

Here, we address this challenge and fabricate stacked metal−dielectric metasurfaces consisting of subwavelength arrays of gold nanorods coupled to silicon nanodisks (Figure 1a) and investigate the optical response and directional radiation properties at near-infrared wavelengths.

A sketch of the considered hybrid metasurface and the meta-atom geometry is shown in Figure 1a,b. A gold nanorod with its fundamental resonance tuned to the design wavelength of 1.1 μm for an electric field polarized along its long axis is used as a feed element. The gold nanorod is placed at a specific distance above a silicon nanodisk featuring strong quadrupolar resonances[22] around the same wavelength. This silicon nanodisk acts as a director element. The metasurface is processed on a SiO_2 substrate with a refractive index of 1.45. The dimensions of the gold rod are l = 180 nm, w = 40 nm, and t = 40 nm. The silicon nanodisk has a height of h = 220 nm and a radius of r = 235 nm and is covered by a 75 nm layer of SiO_2 that acts a spacer layer between the two elements. The spacer layer is optimized to achieve maximum directivity in the forward direction (−z-direction in Figure 1b). The entire structure is embedded into an index-matching oil. In order to produce the metasurface, we arranged the meta-atoms in a two-dimensional array with a lattice constant of a = 670 nm, as shown in Figure 1a.

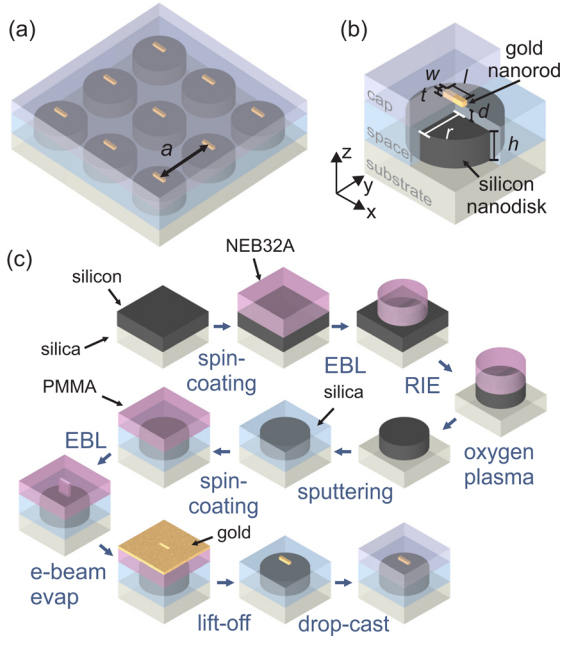

Figure 1. (a) Sketch of the two-dimensional hybrid metasurface and (b) the detailed geometry of a single metal−dielectric nanoantenna. (c) Steps performed for fabrication of the stacked hybrid nanoantenna arrays.

To fabricate the hybrid meta-atoms, we have developed a two-step electron-beam lithography (EBL) procedure, which is schematically illustrated in Figure 1c. The first step of EBL defining the silicon-nanodisk director elements is performed on a silicon-on-insulator wafer (SOITEC) with a silicon layer thickness of 220 nm using the negative-tone e-beam resist NEB-31A. The resulting resist pattern serves as a mask for reactive-ion etching (RIE) of the device layer. Any residual resist is removed by oxygen-plasma etching. In the second step, we concentrate on hybridizing these dielectric elements with the plasmonic gold nanorods in a defined fashion. To this end, we first sputter a thin layer (approximately 5 nm) of indium−tin-oxide (not shown in Figure 1c) to restore the dc conductivity of the sample that has been lost during the etching procedure in the previous step. Next, cross-shaped gold alignment marks are lithographically defined at the corners of the nanodisk arrays, and the sample is carefully mapped in a scanning electron microscope. Note that the latter two steps are not mandatory and have not been depicted in Figure 1c, as alignment markers can also be directly incorporated into the first EBL step. Next, we deposit a thin, 75 nm layer of SiO_2 as a spacer defining the separation distance between the feed element (gold nanorod) and the director element (silicon nanodisk).

We then perform the second step of EBL, defining the gold nanorod feed elements using the positive-tone electron-beam resist PMMA 950 K A4 from Microchem. The predefined marks enable the precise alignment of the second exposure step with regard to the predefined silicon nanodisks. Following exposure and development, we deposit 40 nm of gold via electron-beam evaporation and we perform a lift-off procedure in hot acetone. As a last step, in order to ensure that the resulting structures are situated in an isotropic, low-refractive-index environment during measurement, we drop-cast an index-matching oil (n = 1.45) onto the sample. Alternatively, the application of a thick SiO_2 layer can be considered to provide a homogeneous dielectric environment. A scanning electron micrograph of the resulting nanoantennas before drop-casting the oil is displayed in Figure 2. The inset shows a close-up of a few hybrid nanoantennas in the array.

In the following, the fabricated structures are optically characterized, the measured spectra are compared to numerical simulations, and the directional radiation properties of the hybrid antenna design are studied. For optical characterization we perform linear-optical transmittance measurements using a home-built white-light spectroscopy setup that employs a tungsten-halogen lamp as a light source. By inserting a linear polarizer behind the light source we can choose the electric-field polarization of the incident light to be aligned parallel or

DOI: 10.1021/acsphotonics.6b00012
ACS Photonics 2016, 3, 349−353

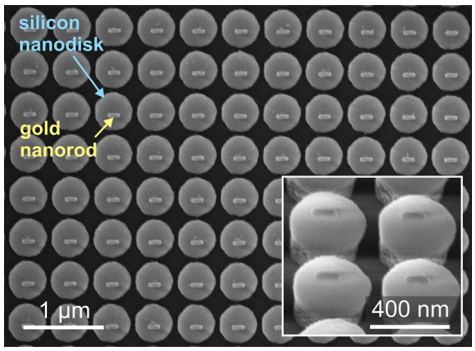

Figure 2. Scanning electron micrograph of the fabricated hybrid metal–dielectric metasurface. The inset shows a magnified and oblique view of the same sample.

perpendicular to the long axis of the gold nanorod, respectively. This allows us to selectively excite the nanorod resonance at approximately 1.1 μm wavelength only for the polarization parallel to the long axis of the gold nanorod. An aperture is introduced in an additional image plane behind the sample to select the light that is passing through the metasurface only. All measurements are referenced to an unstructured sample area of equal size next to the metasurface. The measurement results are displayed in Figure 3a. A significant difference between the

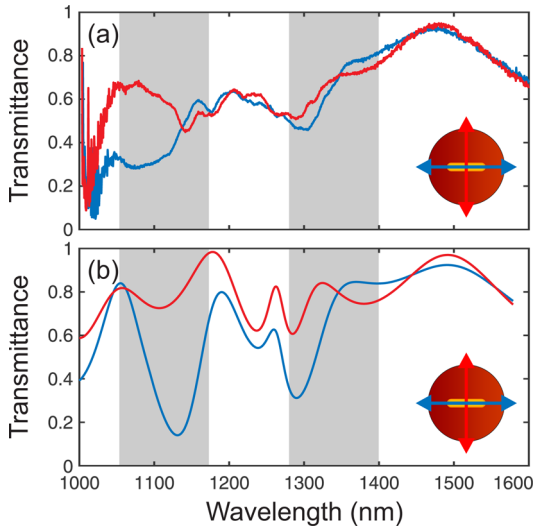

Figure 3. (a) Measured and (b) numerically calculated normal-incidence linear-optical transmittance spectra for incident light polarized parallel (blue) and perpendicular (red) to the long axis of the gold nanorod. The interplay of the plasmonic and the dielectric nanoantenna elements results in a significant difference between the transmittance for the two incident polarizations for the spectral region where the nanorod resonance is excited but also for the off-resonant case at 1.3–1.4 μm wavelength.

transmittance of the metasurface for the two incident polarization directions is observed in the spectral region around the operation wavelength of the nanorod at 1.1–1.2 μm wavelength and in a second spectral region at 1.3–1.4 μm wavelength as well. Since the silicon material tends to be notably lossy below a wavelength of 1 μm, the experimental spectra become noisy when the wavelength approaches 1 μm.

In order to provide an explanation for the observed spectral behavior, we compare our experimental results with numerical finite-integral frequency-domain calculations using the commercial software package CST Microwave Studio. In these simulations the nominal geometry of the fabricated sample has been fully considered. For the optical properties of gold we use the data from ref 23, and for silicon we consider a refractive index of 3.5, respectively. Calculated transmittance spectra for the two linear polarizations are displayed in Figure 3b, showing good qualitative agreement with the experimental spectra. We note, however, that the difference in the transmittance for the two orthogonal polarizations is less pronounced in the experimental spectra as compared to the numerical ones. This is mainly due to sample imperfections, such as imperfections in the alignment of the plasmonic nanorod with respect to the center of the silicon nanodisk.

To shed light on the directional radiation properties of the hybrid metasurface, we furthermore calculate the radiation cross-section of the corresponding single metal–dielectric meta-atom (Figure 4a) and calculate the radiation pattern at

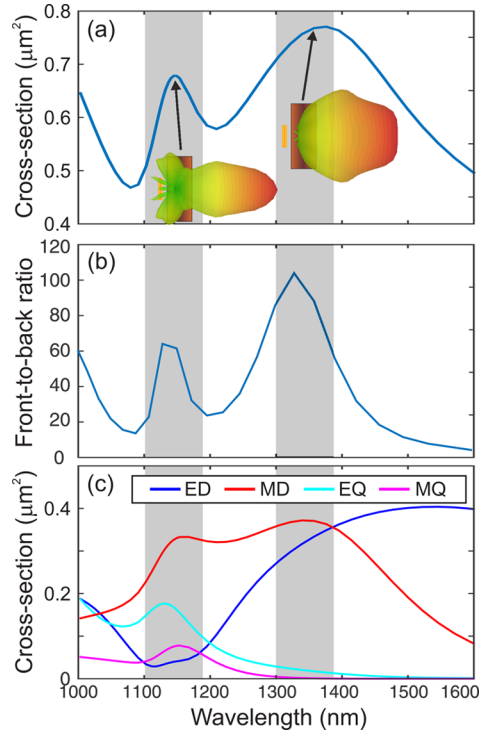

Figure 4. (a) Numerically calculated radiation cross-section for a single metal–dielectric nanoantenna and (b) the calculated front-to-back ratio of the light radiated by the hybrid nanoantenna for incident polarization along the long axis of the gold nanorod. (c) Multipole decomposition of the local fields composed of electric dipole (ED), magnetic dipole (MD), electric quadrupole (EQ), and magnetic quadrupole (MQ) contributions. The insets in (a) show the radiation patterns at the spectral positions marked by the arrows.

the two resonance positions. We additionally calculate the front-to-back ratio (Figure 4b) defined here as the radiated power in the forward direction ($-z$-direction in Figure 1b) divided by the radiated power in the backward ($+z$-) direction. The obtained front-to-back ratio for the two relevant spectral regions is above 60 and 100, respectively. We note that the occurrence of the characteristic radiation properties shown in Figure 4a,b can, in principle, be qualitatively explained by a superposition of the electric and magnetic dipoles of the silicon nanodisk[10,12] and the electric dipole of the gold nanorod that is displaced by 185 nm in the $+z$-direction from the overlapping

DOI: 10.1021/acsphotonics.6b00012
ACS Photonics 2016, 3, 349–353

dipoles of the nanodisk. However, due to interactions in the system, this picture does not reflect the quantitative radiation properties shown in Figure 4a,b. Nevertheless, to study the scattering properties of such a hybrid device, we perform a multipole decomposition of the local fields of a single metal−dielectric meta-atom to identify the multipole components that give rise to the characteristic radiation properties. In the multipole analysis we consider a situation in the simulation where the antenna is illuminated by a plane wave according to the experimental situation. We use again CST Microwave Studios to solve the full wave problem and to extract the scattered field. The scattered field is afterward projected onto the different spherical harmonics, which represent eventually the fields of electric and magnetic dipoles and quadrupoles. This allows extracting the multipole moments induced in the antenna by the respective illumination, and to calculate the contribution of each multipole moment to the scattering cross-section.Thereby it allows quantifying the importance of each multipole moment and provides an excellent base to understand the ability of the hybrid antenna to preferentially scatter the light in the forward direction. More details on the multipole analysis can be found in ref 25. Using this method, we extract the dominating multipole contributions with respect to the central coordinate of the silicon nanodisk from the local near-fields of the meta-atom and plot them in Figure 4c. From Figure 4c we can identify that at wavelengths from 1.1 to 1.2 μm, i.e., when the plasmonic nanorod is in resonance, the directional radiation is caused by the superposition of a pronounced magnetic dipolar contribution with electric (and weaker magnetic) quadrupolar components of the combined system in accordance with previous theoretical findings, where a directional radiation behavior has been attributed to the superposition of electric and magnetic multipole moments in plasmonic nanoantennas.[5] We note that, even though the plasmonic nanorod has a scattering response that is purely electric dipolar, the scattered field from the nanorod in the hybrid design is expanded with respect to a central coordinate that is outside of the nanorod; that is, it is in the center of the silicon nanodisk. Therefore, additional multipole moments than the electric dipole moment are necessary to describe the scattered field of the gold nanorod. In this specific situation the displacement, however, is small and the scattered field is well described by those multipole moments depicted in Figure 4c. Nevertheless, when exploring the ability to suppress the backscattering from those hybrid nanoantennas using, for example, generalized Kerker conditions, the characteristic radiation pattern shown in the inset of Figure 4a can be explained by the superposition of the corresponding multipole components.[24] As such, although the front-to back ratio is higher at the longer-wavelength resonance, the scattering pattern becomes more directive at the resonance of the plasmonic nanorod due to this excitation of higher-order multipoles in the nanodisk.

In contrast to this, the spectral region from 1.3 to 1.4 μm wavelength is dominated by a superposition of the electric and magnetic dipole components of the nanodisk director element that ultimately gives rise to unidirectional radiation with the corresponding characteristic radiation pattern shown in the inset of Figure 4a. Remarkably, in this regime the hybrid meta-atom acts as a Huygens' element[12] and could, therefore, be also used as a fundamental building block for efficient wave-shaping devices.

CONCLUSION

In conclusion, we have realized a hybrid metal−dielectric metasurface composed of gold nanorods that are coupled to silicon nanodisks. To this end, we have implemented and successfully demonstrated a multilayer fabrication approach to realize stacked metal−dielectric meta-atoms that combine the advantages of both plasmonic and dielectric elements. We have studied the optical properties of this metasurface and investigated its directional radiation properties. We show that our design supports unidirectional radiation of light with a maximum front-to-back ratio of above 100 and analyzed the interplay of its multipolar electric and magnetic contributions that lead to the directed radiation behavior of the single constituent elements. In particular, we have identified the operation band where the meta-atoms effectively behave as Huygens' elements that, in principle, allow for full 2π phase manipulation. Therefore, our hybrid metasurface can be used in a range of photonic applications, including wavefront manipulation, directional nanoscale light sources, biosensing, or optical switching and routing.

ASSOCIATED CONTENT

Supporting Information

The Supporting Information is available free of charge on the ACS Publications website at DOI: 10.1021/acsphotonics.6b00012.

Multipole expansions for a single gold nanorod and a single silicon nanodisk (PDF)

AUTHOR INFORMATION

Corresponding Author

*E-mail: isabelle.staude@uni-jena.de.

Notes

The authors declare no competing financial interest.

ACKNOWLEDGMENTS

This work was performed, in part, at the Center for Integrated Nanotechnologies, an Office of Science User Facility operated for the U.S. Department of Energy (DOE) Office of Science. Sandia National Laboratories is a multiprogram laboratory managed and operated by Sandia Corporation, a wholly owned subsidiary of Lockheed Martin Corporation, for the U.S. Department of Energy's National Nuclear Security Administration under Contract No. DE-AC04-94AL85000. The authors also acknowledge support from the Australian National Fabrication Facility (ANFF) ACT node, the Australian Research Council through Discovery Project and DECRA Fellowship grants, and the Group of Eight: Australia−Germany Joint Research Cooperation Scheme and the German National Merit Foundation. I.S. gratefully acknowledges financial support by the Thuringian State Government within its ProExcellence initiative (ACP2020). C.R. thanks the German Science Foundation (project RO 3640/7-1) for financial support. The work was further supported by the DAAD (PPP Australien). We acknowledge the support of the Erasmus Mundus NANOPHI project, contract number 2013 5659/002-001.

REFERENCES

(1) Yu, N.; Capasso, F. Flat optics with designer metasurfaces. *Nat. Mater.* **2014**, *13*, 139−150.

DOI: 10.1021/acsphotonics.6b00012
ACS Photonics 2016, 3, 349−353

(2) Minovich, A. E.; Miroshnichenko, A. E.; Bykov, A.; Murzina, T.; Neshev, D. N.; Kivshar, Yu. S. Functional and nonlinear optical metasurfaces. *Laser & Photonics Rev.* **2015**, *9*, 195−213.
(3) Curto, A. G.; Volpe, G.; Taminiau, T. H.; Kreuzer, M. P.; Quidant, R.; van Hulst, N. F. Unidirectional emission of a quantum dot coupled to a nanoantenna. *Science* **2010**, *329*, 930.
(4) Biagioni, P.; Huang, J. S.; Hecht, B. Nanoantennas for visible and infrared radiation. *Rep. Prog. Phys.* **2012**, *75*, 024402.
(5) Hancu, I. M.; Curto, A. G.; Castro-López, M.; Kuttge, M.; van Hulst, N. F. Multipolar interference for directed light emission. *Nano Lett.* **2014**, *14*, 166−171.
(6) Kruk, S. S.; Decker, M.; Staude, I.; Schlecht, S.; Greppmair, M.; Neshev, D. N.; Kivshar, Y. S. Spin-polarized photon emission by resonant multipolar nanoantennas. *ACS Photonics* **2014**, *1*, 1218−1223.
(7) Taminiau, T. H.; Stefani, F. D.; van Hulst, N. F. Enhanced directional excitation and emission of single emitters by a nano-optical Yagi-Uda antenna. *Opt. Express* **2008**, *16*, 16858−16866.
(8) Krasnok, A. E.; Miroshnichenko, A. E.; Belov, P. A.; Kivshar, Y. S. All-dielectric optical nanoantennas. *Opt. Express* **2012**, *20*, 20599.
(9) Person, S.; Jain, M.; Lapin, Z.; Sáenz, J. J.; Wicks, G.; Novotny, L. Demonstration of zero optical backscattering from single nanoparticles. *Nano Lett.* **2013**, *13*, 1806.
(10) Staude, I.; Miroshnichenko, A. E.; Decker, M.; Fofang, N. T.; Liu, S.; Gonzales, E.; Dominguez, J.; Luk, T. S.; Neshev, D. N.; Brener, I.; Kivshar, Y. S. Tailoring directional scattering through magnetic and electric resonances in subwavelength silicon nanodisks. *ACS Nano* **2013**, *7*, 7824.
(11) Krasnok, A. E.; Simovski, C. R.; Belov, P. A.; Kivshar, Y. S. Superdirective dielectric nanoantennas. *Nanoscale* **2014**, *6*, 7354.
(12) Decker, M.; Staude, I.; Falkner, M.; Dominguez, J.; Neshev, D. N.; Brener, I.; Pertsch, T.; Kivshar, Y. S. High-Efficiency Dielectric Huygens' Surfaces. *Adv. Opt. Mater.* **2015**, *3*, 813−820.
(13) Devilez, A.; Stout, B.; Bonod, N. Compact metallo-dielectric optical antenna for ultra directional and enhanced radiative emission. *ACS Nano* **2010**, *4*, 3390.
(14) Rolly, B.; Stout, B.; Bonod, N. Boosting the directivity of optical antennas with magnetic and electric dipolar resonant particles. *Opt. Express* **2012**, *20*, 20376.
(15) Zeng, X.; Yu, W.; Yao, P.; Xi, Z.; Lu, Y.; Wang, P. Metallo-dielectric hybrid antenna for high Purcell factor and radiation efficiency. *Opt. Express* **2014**, *22*, 14517.
(16) Rusak, E.; Staude, I.; Decker, M.; Sautter, J.; Miroshnichenko, A. E.; Powell, D. A.; Neshev, D. N.; Kivshar, Y. S. Hybrid nanoantennas for directional emission enhancement. *Appl. Phys. Lett.* **2014**, *105*, 221109.
(17) Guo, R.; Decker, M.; Staude, I.; Neshev, D. N.; Kivshar, Y. S. Bidirectional waveguide coupling with plasmonic Fano nanoantennas. *Appl. Phys. Lett.* **2014**, *105*, 053114.
(18) Guo, R.; Decker, M.; Setzpfandt, F.; Staude, I.; Neshev, D. N.; Kivshar, Y. S. Plasmonic Fano nanoantennas for on-chip separation of wavelength-encoded optical signals. *Nano Lett.* **2015**, *15*, 3324−3328.
(19) Shopova, S. I.; Rajmangal, R.; Holler, S.; Arnold, S. Plasmonic enhancement of a whispering-gallery-mode biosensor for single nanoparticle detection. *Appl. Phys. Lett.* **2011**, *98*, 243104.
(20) Noskov, R. E.; Krasnok, A. E.; Kivshar, Y. S. Nonlinear metal-dielectric nanoantennas for light switching and routing. *New J. Phys.* **2012**, *14*, 093005.
(21) Decker, M.; Staude, I.; Shishkin, I. I.; Samusev, K. B.; Parkinson, P.; Sreenivasan, V. K.; Minovich, A.; Miroshnichenko, A. E.; Zvyagin, A.; Jagadish, C.; Neshev, D. N.; Kivshar, Y. S. Dual-channel spontaneous emission of quantum dots in magnetic metamaterials. *Nat. Commun.* **2013**, *4*, 2949−10.
(22) Habteyes, T. G.; Staude, I.; Chong, K. E.; Dominguez, J.; Decker, M.; Miroshnichenko, A. E.; Kivshar, Y. S.; Brener, I. Near-field mapping of optical modes on all-dielectric silicon nanodisks. *ACS Photonics* **2014**, *1*, 794.
(23) Johnson, P. B.; Christy, R. W. Optical constants of the noble metals. *Phys. Rev. B* **1972**, *6*, 4370.
(24) Alaee, R.; Filter, R.; Lehr, D.; Lederer, F.; Rockstuhl, C. A generalized Kerker condition for highly directive nanoantennas. *Opt. Lett.* **2015**, *40*, 2645−2648.
(25) Mühlig, S.; Menzel, C.; Rockstuhl, C.; Lederer, F. Multipole analysis of meta-atoms. *Metamaterials* **2011**, *5*, 64−73.

DOI: 10.1021/acsphotonics.6b00012
ACS Photonics 2016, 3, 349−353